A fast procedure of stress state evaluation in magnetically anisotropic steels with the help of a probe with adjustable magnetizing field direction

Marek Chmielewski, Leszek Piotrowski[1] and Bolesław Augustyniak

Physics Department, Gdansk of University Technology, 80-233 Gdansk, Poland

E-mail: lesio@mif.pg.gda.pl

Received 2 November 2016, revised 10 January 2017
Accepted for publication 20 January 2017
Published 15 February 2017

Abstract

The paper presents a novel approach to the stress state evaluation issue. It deals with a strongly (magnetically) anisotropic materials for which a direct interpretation of the Barkhausen effect (BE) intensity would lead to erroneous results. In such a case one has to take into account both the measured BE intensity and the orientation of the magnetisation direction relative to the magnetic easy axis. For the in plane stress distribution evaluation one has to perform at least three measurements in the non-collinear directions. The application of an apparatus with automatically changing magnetizing field direction allows to obtain the angular distribution of the BE intensity in about 30 s (with the angular step of 10°). Thanks to the dedicated post-processing software the procedure of the measurement data processing, resulting in the full information on the stress distribution (main stress components and their orientation in all the investigated points) is almost instantaneous. Apart from the measurement results the stress determination procedure requires two additional pieces of information. The first one is the calibration data obtained for at least two applied strain directions (along easy and hard magnetisation axes)— the data for the intermediate orientations are usually interpolated. The second one is the 'reference level' of the BE intensity angular distribution. In the case of welded plates it is obtained by averaging the results obtained at the analysed points before welding. The way of results presentation proposed in that paper is very illustrative and shows an interesting feature of the stress distribution in welded plates—namely the appearance of a 'vortex' structure of main stress.

Keywords: Barkhausen effect, magnetic anisotropy, stress distribution, welding

1. Introduction

Fast, cost effective evaluation of the stress distribution in the steel components is a crucial issue for the non-destructive diagnostics of industrial installations. It is especially important for the high pressure steam pipelines or heavily loaded components (tanks, girders etc). The surface stress components i.e. the values and directions of the main stresses (σ_1, σ_2) may be determined with the help of the hole drilling method, or x-ray diffraction analysis [1]. The information obtained in such a way is 'local' and the measurement time in both cases is relatively long. Being so, neither one of those methods can be recommended for the analysis of the spatial distribution of the stress state (obtaining a dense enough matrix of data in an acceptable amount of time). The search for the method that

[1] Author to whom any correspondence should be addressed.
Gdansk University of Technology, Faculty of Applied Physics and Mathematics, Narutowicza 11/12, 80-233 Gdańsk, Poland.

could be applied for such task is thus fully justified. One of such methods, that seem to be well suited for that purpose, is based on Barkhausen effect (BE) signal intensity measurements [2]. The BE signal is due to the abrupt magnetic flux changes inside the material caused by the discontinuous motion of domain walls (DW). The discontinuity is due the pinning/unpinning of DWs on the material's inhomogeneities (grain boundaries, precipitates, dislocation tangles). The application of the external stress modifies the domain structure of the material thus resulting in the change of the BE signal intensity. Tensile stress tends to increase the BE signal whereas the compression results in the decrease of that signal. This is also true for the residual stress (e.g. due to grinding [3] or plastic deformation [4]). Typically measurements are performed with the help of a probe consisting of a single small electromagnet and a detection probe placed between its legs. The measurement lasts several seconds and as a result one obtains the information on the elastic deformation of the material in the direction parallel to the magnetisation direction (probe axis) [5]. However, in order to determine the stress state in the given point one has to find the direction of the main stress (σ_1) and to do that in a reliable way one has to measure the angular distribution of the BE signal. To achieve that, applying a typical probe (unidirectional), one has to repeat the measurements, changing manually the probe orientation [6]. Much better solution is the application of the probe capable of an automatic change of the magnetic field direction. In the literature there have been described BE probes with two perpendicular cores [7, 8] and magnetising coils fed with the currents phase shifted by 90°. Such a probe generates the rotating magnetic field that results in the angle dependent BE intensity measurements. To a some degree such measurements can give information on the magnetic anisotropy of the samples yet due to completely different magnetisation dynamics in such configuration the issue of calibration that could allow for the stress determination remains open. The probe proposed by our group works in an analogous way to the unidirectional probe (the magnetisation direction during the BE signal intensity measurement is constant and as soon as it is done the new orientation is set) and the results obtained that way can be much more easily interpreted. What is important, the automation of the field axis adjustment results in the very fast measurements—one full field axis rotation takes about 30 s. The preliminary results obtained with the help of the abovementioned probe have been already published for the case of an isotropic material [9]. The results of the numerical calculations of the flux distribution in the material magnetised by such a probe have also been discussed in [10]. Now we would like to tackle much more ambitious task i.e. the issue of anisotropic (magnetically) materials.

In the previous article [9] some general information concerning the application of the probe with rotating field direction for the investigation of welded plates made of isotropic steel was given. Now we would like to present some details of the probe and its performance and describe in detail the procedure enabling the main stresses determination on the basis of the BE signal angular distribution obtained for the anisotropic material. As it was in the earlier paper, the investigated object was the welded plate, yet in this case it was made of high strength steel (Polish grade S460M—EN 10025-4:2004) which displayed very pronounced BE intensity anisotropy with the highest BE intensity direction parallel to the rolling direction.

2. Probe description

The schematic view of the BE probe is shown in figure 1. The ferritic core (1) is used in order to increase the magnetic flux changes caused by the domain wall movements in the close-to-surface region of the investigated materials. It results in a significantly higher values of the voltage induced in the detecting coil (2) (BE voltage signal). The change of magnetisation of the material is performed with the help of two perpendicular electromagnets. As can be seen in figure 1 the probe consists of two C-shaped cores (3) and four magnetising coils (4). The yokes have a square cross-section (10x10 mm) and the distance between yoke legs centres is 30 mm. The mounting of the cores, thanks to the springs (5), enables relative movement of the one of the cores in the direction perpendicular to the investigated surface. The ferrite core and the detecting coil are also moveable and as a result the probe can be mounted on the curved surfaces such as e.g. pipes or tanks. The calculation (described in [10]) showed that the applied electromagnet's yoke cross section is big enough to obtain flux densities in the material below the central point of the probe of the order of 1–1.5 T (despite the observed flux leakage effects).

The BE probe is controlled by the electronic measurement device (MEB 2D) and a PC computer equipped with the dedicated LabVIEW based software. The device consists of the magnetising current generator (triangular in form, $f = 10$ Hz), BE voltage signal amplifiers (with adequate band-pass filters operating in the range 5–100 kHz) and a fast (2MS/s) measurement card (16 bit resolution). The magnetising currents amplitudes (I_x and I_y) are changed in such a way that the resulting magnetisation direction is set at the chosen angle (φ) relative to the probe axis (parallel to the fixed core). Figure 2 presents the results of the measurements obtained with the help of a Hall effect probe placed in the central point between the probe legs in such a way that it measured a planar component of the magnetic induction. The orientation of the Hall probe was changed by a step motor with the increment of 10°. The figure depicts the magnetic induction angular distribution for one period of magnetisation obtained for the ratio of the magnetising currents I_x:I_y = 1:2. As can be seen, the most pronounced changes in the magnetic field intensity are observed for the angle φ close to 63° what is very close to the expected result being the value of the expression $\varphi = \arctan(I_y/I_x)$. For the given ratio of the magnetising currents amplitudes, the BE intensity measurement is performed and then the ratio is changed in order to obtain the new magnetising field orientation. On the basis of the measured BE noise signal, its short-time rms envelopes are calculated ($Ub(t)$) and recorded. From the obtained envelopes the peak to peak values are determined (Ubpp) and the integrals (IntUb) over one magnetisation period (after the noise level subtraction)

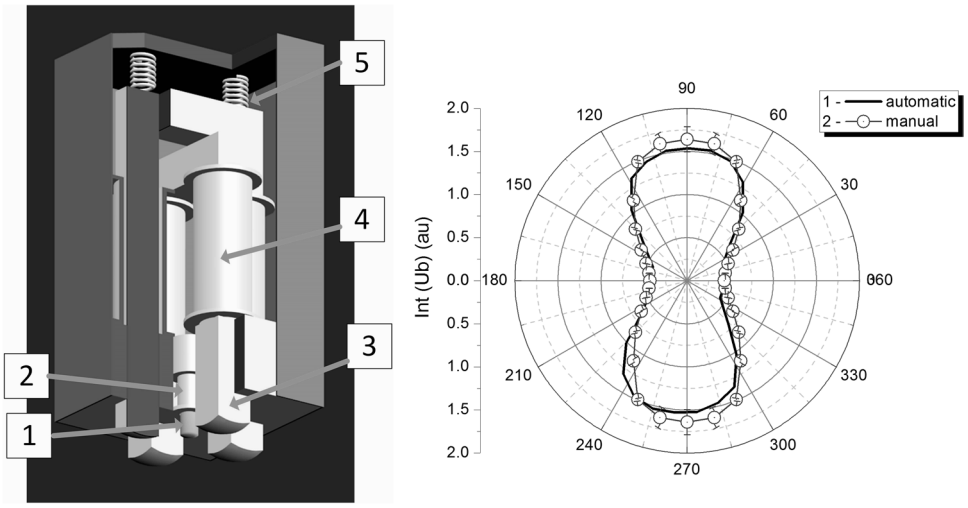

Figure 1. Schematic view of the BE probe (left) and the comparison (right) of the angular BN intensity distribution obtained with the rotation of the field axis (plot 1) and manual rotation of the probe (plot 2).

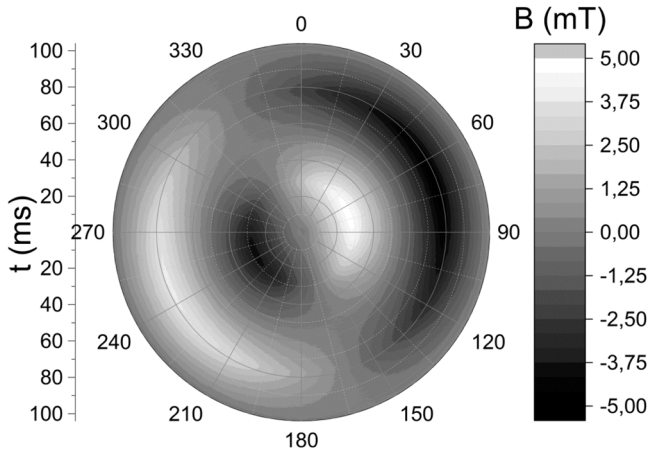

Figure 2. Angular distribution of magnetic field intensity in the central point between the poles of the probe electromagnets during one period of magnetisation. Magnetising currents ratio 1:2.

are calculated. The later ones (being more stable) are then used as a synthetic measure of the BE signal intensity for a given value of the φ angle. The polar plots IntUb(φ) give the information on the anisotropy of the material as well as on the stress level. It should be stressed that the measurement time is very short and for the angular step $\Delta\varphi = 10°$ it takes about 30 s to perform a full rotation. The BN intensity measurements performed with the rotating magnetizing field axis (plot 1) were compared with the ones made by manual rotation of the probe and uniaxial magnetisation (plot 2)—the results are shown in the right part of the figure 1—as can be seen the agreement is very good.

3. Investigated material

The experiment described in the paper was performed on the welded plates made of high strength steel S460ML (EN 10025-4:2004—chemical composition is given in table 1) displaying strong magnetic anisotropy. The BE intensity obtained for the rolling direction was about two times higher than in the perpendicular direction. Such behaviour results probably from the fact that the grains in that steel are strongly elongated in the rolling direction. Such elongated grains are more easily magnetised (due to lower demagnetising effects) in the main axis direction. The as-delivered sheets had the thickness $h = 15$ mm and from the sheets the plates of the following dimensions: length $L = 500$ mm and width $W = 150$ mm, were cut out for welding. The welding was performed with the help of multi-pass MAG method and the chamfering type was *X*.

4. Calibration procedure

Calibration procedure is necessary in order to determine the dependence of the BE intensity on the elastic strain level in the case of two axial stress distribution [11]. The calibration was performed on a cross shaped sample (cross span was 200 mm and the cross arms width 50 mm) cut out from the investigated sheets. The strain level in the central part of the cross was changed by four-point bending of the cross arms. The magnitude of the strain was determined with the help of tensometric rosette glued on the opposite side of the sample. The application of the rosette, by the control of the third strain component, allowed for the verification if the main strain components lie along the sample arms. In figure 3 there are plotted angular distributions of the BE signal intensities obtained for the chosen values of strains ε_x and ε_y (applied either in the direction parallel $\varphi = 0°$ or perpendicular $\varphi = 90°$ to the rolling direction). The calibration was performed in the range of strain from $\varepsilon = -800 \cdot 10^{-6}$ up to $\varepsilon = 800 \cdot 10^{-6}$. The strong magnetic anisotropy of the material results in the strong elongation of the BE intensity angular distribution obtained for the non-deformed sample (figure 3 plot 1).

In figure 4 there are presented two plots illustrating the dependence of the BE signal intensity, measured in the rolling direction and the perpendicular direction, on the strain level applied parallel to the measurement direction. As can be seen,

Table 1. Chemical composition of S460ML steel (EN 10025-4:2004).

Element	C	Mn	Si	P	S	Al	Nb	V	Ti	Cr	Mo	Ni	Cu	N
Max. (wt%)	0.16	1.7	0.60	0.025	0.025	0.02	0.05	0.12	0.05	0.30	0.20	0.80	0.55	0.025

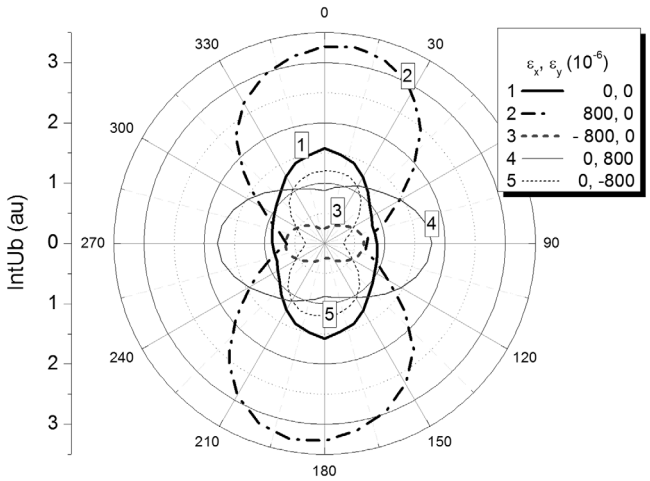

Figure 3. Angular distributions of the BE signal intensity for the chosen strain values (ε_x and ε_y).

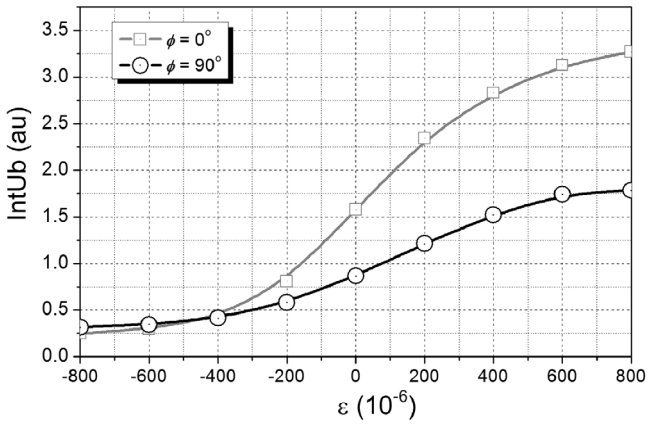

Figure 4. The dependence of the BE signal intensity on the strain measured along the easy ($\varphi = 0°$) and hard ($\varphi = 90°$) magnetisation directions.

the BE signal intensity strongly increases during tension (parallel to the measurement direction) and decreases during compression. Such changes can be explained by the magnetoelastic effects leading to the magnetic domain structure modification [5]. Tensile stress leads to the increase of population of magnetic domains with magnetisation direction oriented in the direction parallel to the stress direction, whereas compressive stresses increase the population of the domains oriented in the direction perpendicular to the applied stress. Being so, it is easier to change the magnetisation state of the material by applying the magnetic field in the direction parallel to the tensile stress. As a results the BE signal intensity is higher when the direction of the tensile stress is parallel to the magnetisation direction and lower in the case of compressive stresses in the same direction. One must however realise that the BE intensity is material specific due to the differences in the microstructure of steels (grain size, precipitate distribution and size). Being so, for every steel grade the calibration has to be performed separately.

From the practical point of view, the more important is the reversed dependence i.e. the dependence of the strain level ε on the relative changes of the BE signal intensity (IntUb). It is better to use the relative changes of the BE intensity (instead of the absolute ones) for two reasons. Firstly the relative changes for two perpendicular directions (easy and hard) are much more similar than the absolute ones. Secondly such curves can be used for the various batches of the same steel with higher accuracy since small changes of the signal observed for non-deformed samples typically do not affect relative changes very strongly. Relative changes are determined in a simple way:

$$\mathrm{IntUbn}(\varepsilon) = \frac{\mathrm{IntUb}(\varepsilon)}{\mathrm{IntUb}(\varepsilon = 0)}, \tag{1}$$

where $\mathrm{IntUb}(\varepsilon)$ is the BE signal intensity measured for the given strain value and the $\mathrm{IntUb}(\varepsilon = 0)$ is the BE intensity obtained for the unloaded sample. The set of curves obtained for the calibrated sample is shown in figure 5. As can be observed the normalised curves are quite similar, what is not surprising as it was already shown that with the proper normalisation procedure one gets similar curves for significantly different materials [12]. Two curves, for the angles $\varphi = 0°$ and $\varphi = 90°$ are the ones that are directly measures during the calibration process. The remaining ones are calculated on the basis of those two curves. They are generated with the raster equal to the angular step ($\Delta\varphi = 10°$) applied during the measurements. The function that was chosen for the generation of the intermediate curves had the form: $Y(\varphi) = Y(90) + \Delta Y \cos^2\varphi$, where $\Delta Y = Y(0) - Y(90)$ is the difference between the BE intensity obtained for the measurements parallel and perpendicular to the easy magnetisation axis. The transition function $\cos^2\varphi$ has been chosen arbitrarily, yet such dependence is observed for the magnetocrystalline energy distribution in the case of uniaxial anisotropy materials. Such behaviour of the BN energy was also reported by Krause *et al* during investigation of the stress-dependent magnetic easy axis in steel [13]. It should be stressed that (as mentioned earlier), the obtained normalised curves are very similar, depend weakly on the measurement angle φ (especially for the tensile strain) and being so, the exact transition function is of smaller importance. The calibration data (inverse relations) $\varepsilon(\mathrm{IntUbn}, \varphi)$ are then used for the angular distribution of strain determination. The data are not fitted with any analytical relationship but are saved as a discrete array of elements from which the strain distribution is determined by linear interpolation.

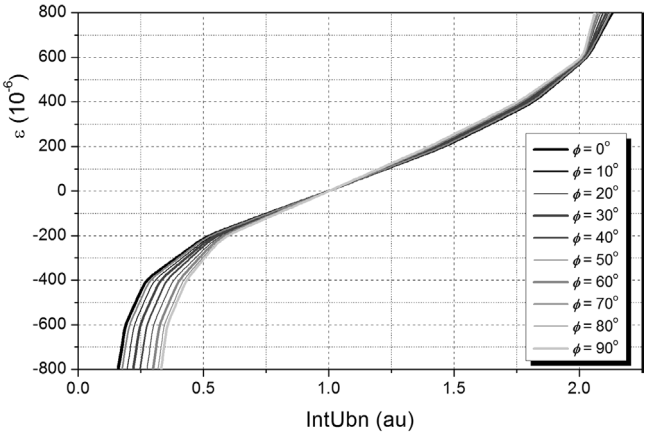

Figure 5. The set of the reverse calibration functions (normalised).

5. The procedure of the determination of strain angular distribution and main stress components

The procedure of local strain (stress) state determination is based on three types of information: (1) angular distribution of the BE intensity $\mathrm{IntUb}(\varphi)_0$ obtained for the unstrained state treated later on as a 'reference level', (2) calibration data $\varepsilon(\mathrm{IntUb}, \varphi)$ and (3) angular distribution of the BE intensity $\mathrm{IntUb}(\varphi)$ measured at the point being investigated. In the case of anisotropic materials the BE probe should be oriented (in respect to the anisotropy axis) in the same way as during calibration procedure. In the paper the $\varphi = 0°$ direction coincides with the easy magnetization axis. The reference angular distribution $\mathrm{IntUb}(\varphi)_0$ is calculated as a mean value from all the measurements performed on the plates (both upper and bottom sides) before welding. Such a mean value is much more representative of the unstrained state than the one used in the calibration procedure. Those two values may be slightly different, since the as-delivered plates may have some residual stress even before welding.

The procedure of local stress state determination consists of four (described below) steps.

(A) Calculation of the normalized BE signal intensity angular distribution $\mathrm{IntUbn}(\varphi)$. In order to do so the as-measured distribution $\mathrm{IntUb}(\varphi)$ is divided by values obtained for the 'reference state' $\mathrm{IntUb}(\varphi)_0$.

(B) Calculation, for every angle (φ), of the value of the strain $\varepsilon(\varphi)$ on the basis of the obtained earlier reverse calibration data $\varepsilon(\mathrm{IntUbn}, \varphi)$. The exact strain values are calculated with the help of linear approximation of the calibration data array.

(C) Determination of the ε_x and ε_y components of the strain distribution and of the main strain axis orientation. The ε_x and ε_y components are given by the values $\varepsilon(\varphi = 0°)$and $\varepsilon(\varphi = 90°)$ respectively. The main strain axis orientation (the angle α relative to the x axis) is obtained with the help of a fitting procedure (Levenberg–Marquardt algorithm) applied to the $\varepsilon(\varphi)$ distribution with the fitting function of the form:

$$\varepsilon_\phi = \varepsilon_2 + (\varepsilon_1 - \varepsilon_2)\cos^2(\phi - \alpha). \tag{2}$$

(D) Calculation of the σ_x and σ_y components of the stress state and main stress components σ_1 and σ_2. The calculations are performed with the help of the Hooke's law assuming 2D (in plane) strain distribution. The Young modulus and Poisson's ratio are assumed to be isotropic. This is a reasonable assumption since mechanical tests (tensile loading) didn't show any measurable mechanical anisotropy. The relations applied are as follows:

$$\sigma_x = \frac{E}{1-\nu^2}(\varepsilon_x + \nu\varepsilon_y);\ \sigma_y = \frac{E}{1-\nu^2}(\varepsilon_y + \nu\varepsilon_x). \tag{3}$$

Using the as obtained components σ_x and σ_y and the angle α (main strain axis orientation, which for the mechanically isotropic material is parallel to the main stress axis) one may calculate the main stresses σ_1 and σ_2 according to the formulae:

$$\sigma_1 = \frac{\sigma_x\cos^2\alpha - \sigma_y\sin^2\alpha}{\cos 2\alpha};\ \sigma_2 = \frac{\sigma_y\cos^2\alpha - \sigma_x\sin^2\alpha}{\cos 2\alpha}. \tag{4}$$

If the measurements are performed for an array of points on the investigated plates, the obtained results may be presented in the form of maps showing the spatial distribution of chosen parameters. Typically the maps of the σ_x and σ_y components are presented where the symbols x and y refer to the orientation in respect to the weld seam, x denotes the parallel orientation and y the perpendicular one. In our paper, in addition to the abovementioned maps, we present the results in a more illustrative way, showing the distribution of σ_1 and σ_2 stresses and their orientation in every point with the help of pairs of vectors representing both the magnitude and orientation of main stresses.

6. Case study—strain and stress distribution determination in the welded plates

An application of the discussed method will be described in the case of welded plates made of magnetically anisotropic steel (with the easy magnetisation axis perpendicular to the seam). The results for one side (upper) of one of the welded plates are presented in detail and a vector plot showing the main stresses distribution for the other side (bottom) is included together with the x-ray data.

Such a task has been already undertaken by various researchers for welded plates made of API 5LX70 [14], AISI 1008 [15] and electrical steel [16]. There have also been made tests on the tubes made of 9Cr-1Mo steel [17]. In all those cases the measurements were unidirectional and thus allowed only for the evaluation of one stress component. There have also been reported investigations of welded plates in which signals in two perpendicular directions were measured (e.g. [18]). The possibility of the stress distribution measurement being confirmed with 'classic' probes we decided to verify the adequateness of our way of measurements for such a task. The measurements of the BE signal intensity angular distribution were performed on both sides of the investigated plates in 25 points on each side. As a result we obtained a 5

by 5 array of results for each plate side. The distance between measurement points in the direction parallel to the weld seam (longer edge of the plate) was 100 mm and in the perpendicular direction 28 mm. The points were labelled with the pairs of coordinates [i, j], where [1,1] stands for the upper left corner, whereas [1, 3] represents the closest point to the weld seam centre. The line is about 25 mm from the edge of the plate—such a relatively big distance is due to the probe dimensions (a smaller version is presently being designed) since the weld seam did not allow for a proper placement of the probe. Being so, the measurements are performed on the base material and the HAZ (heat affected zone) microstructure changes does not have to be taken into account in the stress evaluation process. During the measurements the probe axis was oriented perpendicularly to the longer edge of the plates (along easy magnetisation axis) in order to be in agreement with the calibration conditions. The direct results of the BE intensity angular distribution measurements on the investigated plate surface before welding are shown in figure 6. As can be seen, for most of the investigated points the BE intensity measured in the direction perpendicular to the longer edge (parallel to the rolling direction) is highest. For the direction parallel to that edge, the BE intensity is approximately two times lower. It can also be noted, that the scatter in the obtained results is significant what can suggest the non-uniform distribution of post-rolling residual stresses.

The next figure (figure 7) shows an analogous results (25 BE signal intensity angular distributions) obtained on the same plate, yet after welding. The results for the points closest to the weld seam are located in the upper row of the picture. Comparing the two arrays of results (figures 6 and 7) one can see that the welding process results in a visible rotation of the main axes of the BE intensity angular distributions (away from the $\varphi = 0°$ direction) in the lateral regions of the plate. The change is most pronounced in the close to the seam regions and seems to be symmetrical (the axis of symmetry being perpendicular to the seam). Qualitative analysis of the obtained distributions suggests that the most important feature is the appearance of tensile stresses parallel to the seam in the area close to the seam, what is a common behaviour in the welded plates [19]. Below we discuss the details of subsequent steps leading to the stress components determination in one of the investigated points (point [1, 3]). Firstly, all the distributions shown in figure 6 were averaged and the reference BE intensity distribution was calculated—IntUb(φ)$_0$. Such a distribution is plotted in the figure 8 (plot 1) and, as can be seen, it is somewhat different from the one obtained for the calibrated sample in the unloaded state (figure 3, plot 1) as well as the ones for the investigated point before welding (probably due to non-zero initial strain level). The results obtained for each point on the plate were then normalized according to the procedure described earlier. The results of the BE intensity measurements for the chosen point ([1, 3]) obtained after welding are presented in figure 8 (plot 2).

As can be observed, there is a very pronounced difference between those results and the reference distribution (plot 1), especially in the direction close to the angle $\varphi = 90°$. As a result, the normalised BE intensity distribution—IntUbn(φ) (figure 9, plot 1) is strongly elongated in that direction. Its shape is completely different from the distribution before normalisation what confirms the importance of taking the anisotropy into account during the analysis of the experimental BE data.

The reverse calibration data obtained for the reference sample ε(IntUbn, φ) were used for the determination of the angular distribution of strain $\varepsilon(\varphi)$ for all the investigated points. In the case of the analysed point, the resulting distribution (figure 9, plot 2) is very similar to the normalised BE intensity distribution. It is so, because the strain levels are not very high and correspond to the quasi-linear region of the calibration curves (observed for the IntUbn $\in (0, 5; 2)$). As could be expected on the basis of a qualitative analysis the resulting strain is slightly negative for $\varphi = 0°$, increases for higher angles and reaches its maximum, close to $500 \cdot 10^{-6}$, for $\varphi = 90°$ (for illustration sake, the circle $\varepsilon = 0$ was plotted in figure 9 with a dashed line). The next step was the determination of the main strain axis orientation (α angle) with the help of the fitting procedure mentioned earlier (formula (2)), as can be seen for the analysed point that angle was very close to 90°.

On the basis of the obtained ε_x and ε_y values the σ_x and σ_y stress components were calculated from the formulae (3). The Young modulus was derived from the tensile loading tests and its value was $E = (210 \pm 3)$ GPa, as for the Poisson's ratio it was assumed to be $\nu = 0.3$. Taking into account the determined α angle the main stresses σ_1 and σ_2 were also calculated with the help of formulae (4). The complete set of the calculated values for the analysed point is presented in table 2. The table contains also the analogous data for the point on the opposite (bottom) side of the plate. It can be noted that, due to the almost parallel to the seam orientation of the strain distribution, the σ_1 and σ_2 components are identical (within the accuracy limits) to the σ_x and σ_y ones. It would naturally not be the case for all the points (e.g. [1, 2] or [1, 4]).

The results obtained in an analogous way for all the measured points create a comprehensive set of data describing the stress distribution in the investigated plate. It can be illustrated with the help of maps showing the spatial distribution of the σ_x and σ_y components. The results for the σ_x (parallel) components are presented in figure 10 and figure 11 shows the results for the σ_y (perpendicular) component. The location of the weld seam was shown schematically at the upper edge of the maps. It should be noted that due to the different x and y spacing of the measurement points the scales on the maps axes are not identical. In the figure 10 map one can see that the σ_x component exceeds 100 MPa (tensile stress) in the central part of the close to the seam region. On the other hand strong compressive stresses (~−80 MPa) are observed at the opposite side of the plate. As for the σ_y component (map in figure 11) it is relatively low in the central part of the plate (±20 MPa) and higher values are observed only in the lateral parts of the plate (~−60 MPa).

The as presented maps are illustrative, yet do not give all the information that could be extracted from the angular intensity plots (figures 6 and 7). On their basis, the orientation of the main stress axis cannot be determined. Only in the case of

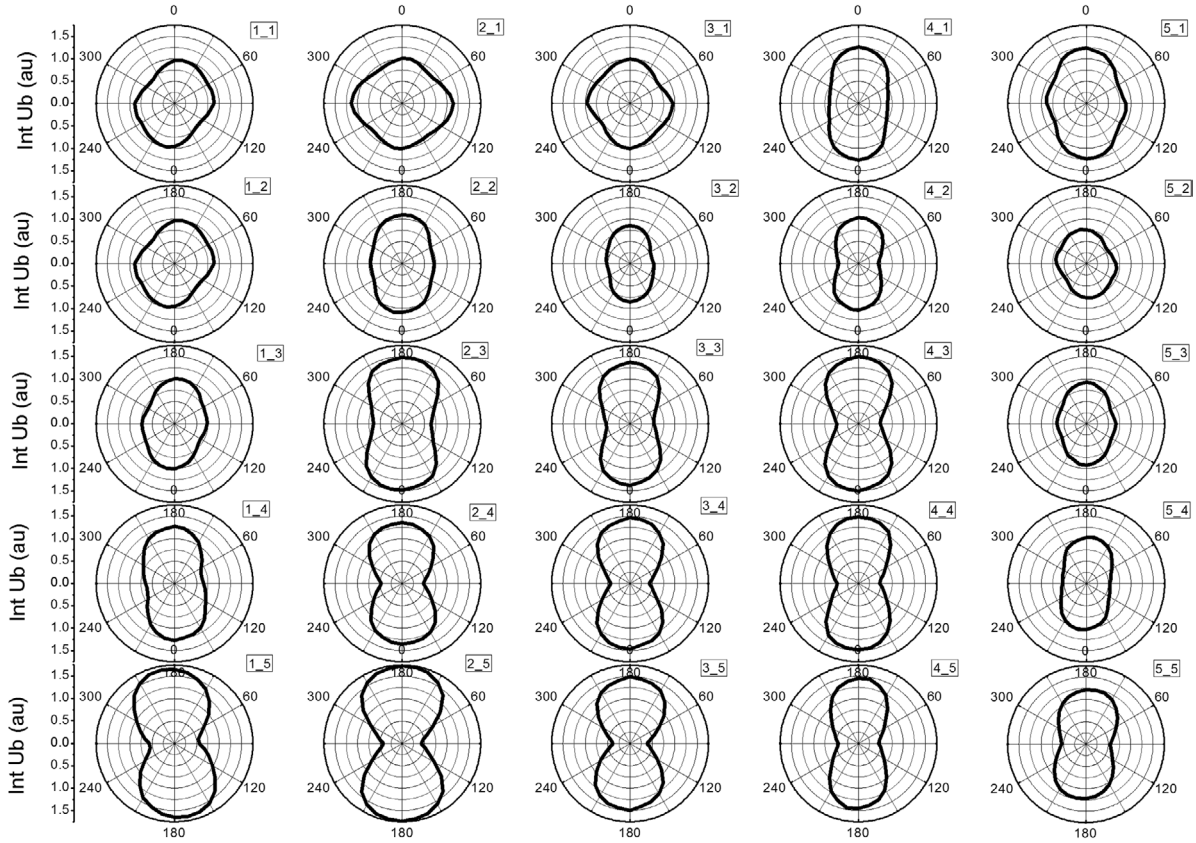

Figure 6. The BE intensity angular distributions measured for the array of points $[i, j]$ on the surface of the investigated plate before welding.

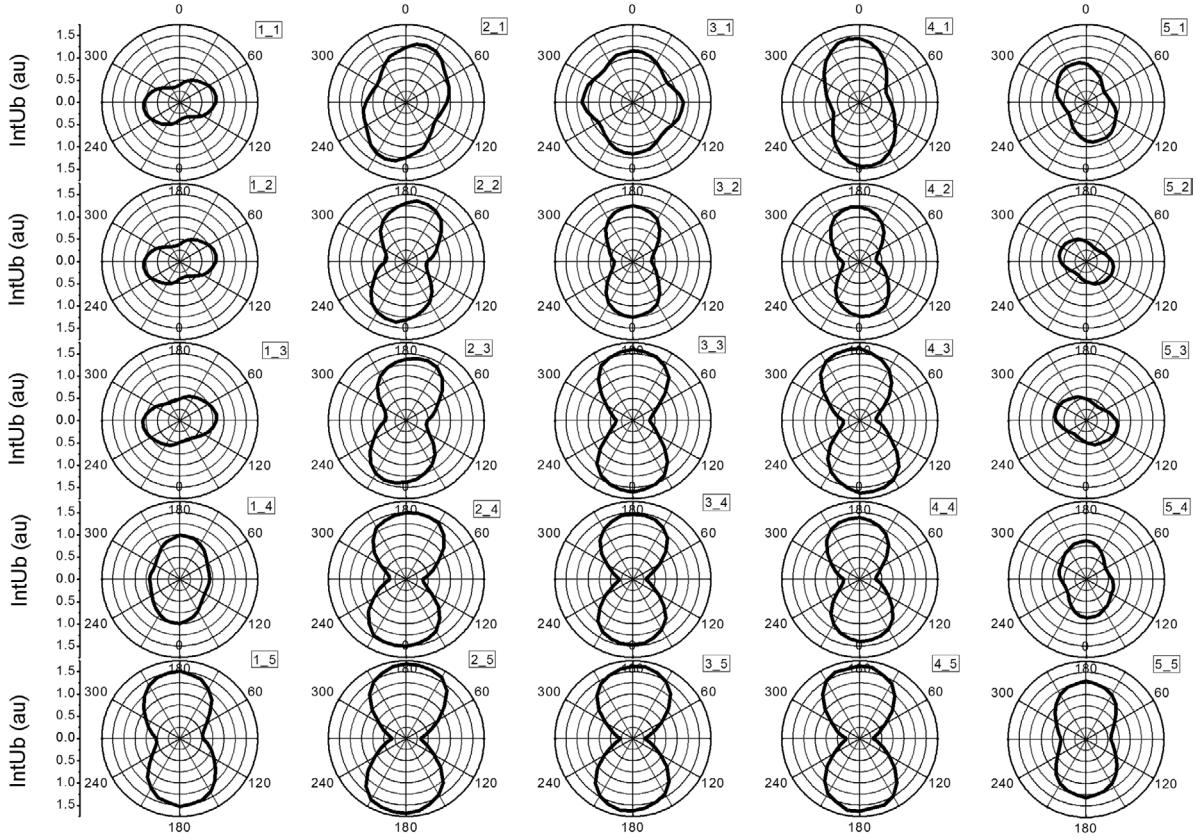

Figure 7. The BE intensity angular distributions measured for the array of points $[i, j]$ on the surface of the investigated plate after welding.

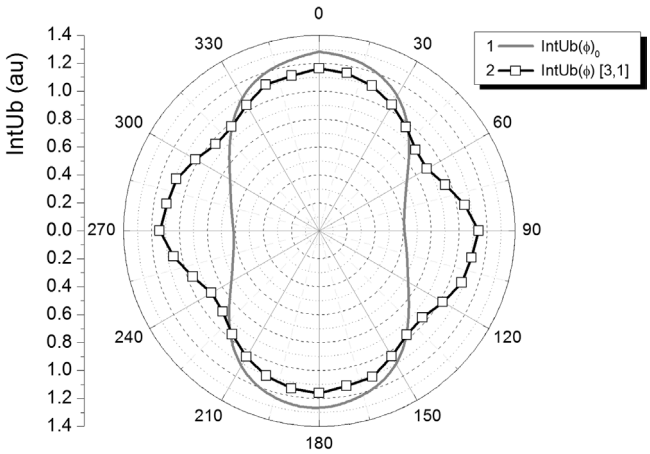

Figure 8. Angular distributions of the BE signal intensity: 1—the averaged value of the results obtained before welding (reference level), 2—the value obtained for the [1, 3] point after welding.

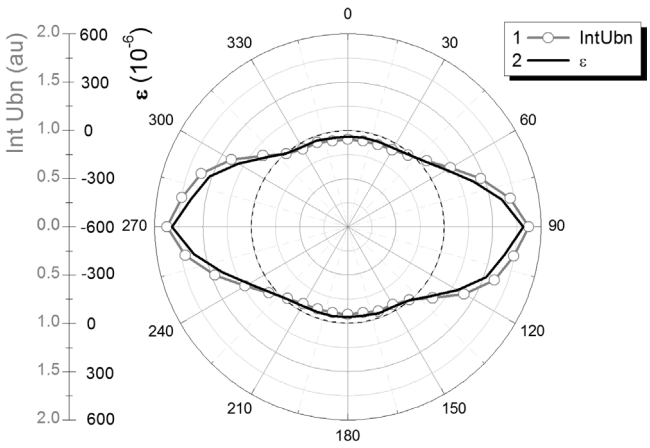

Figure 9. Angular distributions measured for the [1, 3] point after welding: 1—normalised BE intensity, 2—strain ε.

stress axes almost parallel or perpendicular to the plate edges the σ_x and σ_y components are close to the σ_1 and σ_2 ones. If one could *a priori* assume the main stress axis orientation, the presented set of data would be satisfactory (it is e.g. the case of point [1, 3] where on the basis of welding thermodynamics models one expects tension parallel to the seam [20]). In a general case, however, one has to know the set of three values (e.g. σ_1, σ_2, α) and it is not easy to present it in a synthetic graphical way. We propose an original solution to that task—an attempt at such presentation is shown in figure 12. Main stress components are presented with the vectors of different width (the thick one representing the σ_1 component). The vectors either start at the analysed point location (positive, tensile stresses) or point toward it (negative, compressive stresses). The X and Y components refer to the location of the analysed points expressed with the point coordinates coinciding with the ones used in figures 6 and 7. The vector length represents the stress magnitude according to the legend (200 MPa corresponds to unity on spatial scales). The σ_1 and σ_2 vectors are naturally (since they represent main stresses) perpendicular to each other, and the angle α (according to the convention used while calculating table 2 data) is calculated clockwise in respect to the Y axis. Taking as an example the analysed point [1, 3] we have close to the half of the spatial unit vector representing σ_1 component (+115 MPa) starting at the measured location, oriented almost parallel to the seam (−87° in respect to Y axis). As for the vector representing σ_2 it has length of one eights (25 MPa), starts at the analysed point, and is perpendicular to σ_1. Such a way of measurement data presentation is definitely much easier for interpretation as it is 'intuitive'. One can easily see a 'vortex' composed of compressive stresses 'flowing' from upper left corner, through the lower part of the plate to its upper right corner. The origin of such stress distribution is not obvious, yet it was observed on both sides (top and bottom) for several welded plates investigated by our team. Probably it is due to the clamping procedure necessary in order to prevent the plates from shifting during welding. The data for the opposite side of the plate are presented in figure 13 in which a similar distribution of the main stresses is seen. There can also be observed tension in the close to the seam region and the 'vortex' structure is even more pronounced.

One remaining issue to be addressed concerns the accuracy of the measurement and the resulting uncertainty. The accuracy depends strongly on the microstructural similarity of the reference sample to the investigated object. Even though, luckily, the rate of change of the normalized (relative) changes of the BE intensity as a function of applied strain is similar for most of the commercially available steels, choosing for calibration a sample with a significant residual stress level may lead to erroneous results. The repeatability of the BE signal intensity does not influence the resulting accuracy strongly as it typically of the order of 1%. The uncertainty of the ε_x and ε_y components determination results from the calibration curves accuracy, and increases significantly for high strains (where the quasi linear relationship between the strain and BE intensity holds no more). The uncertainty of the $\varepsilon(\varphi)$ determination for angles other than 0° and 90° may be higher since they are determined on the basis of the calibration curves that are not measured but interpolated. However, due to the fact that the relative curves do not differ much and to the fitting procedure that smooths out the scatter in the angular distribution, the α angle should be quite accurate. The additional uncertainty arises from the Young modulus and Poisson's ratio accuracy. Summarising, taking into account all the mentioned uncertainty sources we estimate the uncertainty in the case of stress level in the range ±150 MPa to be of order of 10%. The only problem arises for the case of angle $\alpha = 45°$ (or very close to it). In such a case the denominator in the formulae (4) is equal to zero and we cannot calculate the main stresses. For isotropic materials it can be easily circumvented by rotating the probe and repeating measurements (the control software calculates the BE intensity distribution and main axis orientation, which for the isotropic materials is equal to the strain/stress axis orientation). The observed weak dependence of the obtained BE angular distributions on the probe orientation for such materials is probably due to the fact that the dynamics of the stress induced BE intensity changes is different from the one observed for the magnetic properties and in fact the magnetisation conditions

Table 2. Strain and stress state in the [1, 3] point of the investigated plate (on both sides).

	ε_x (10^{-6})	ε_y (10^{-6})	α (°)	σ_x (MPa)	σ_y (MPa)	σ_1 (MPa)	σ_2 (MPa)
Up	491 ± 10	-39 ± 5	-87 ± 3	111 ± 15	25 ± 5	111 ± 15	25 ± 5
Bottom	538 ± 10	-217 ± 10	-87 ± 3	109 ± 15	-13 ± 5	109 ± 15	-13 ± 5

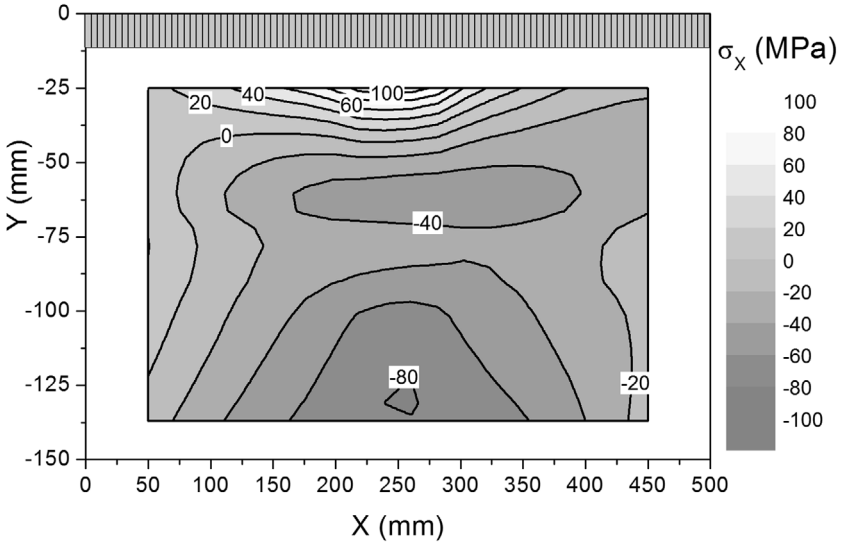

Figure 10. The map showing the σ_x (parallel to the weld seam) component distribution on the investigated plate.

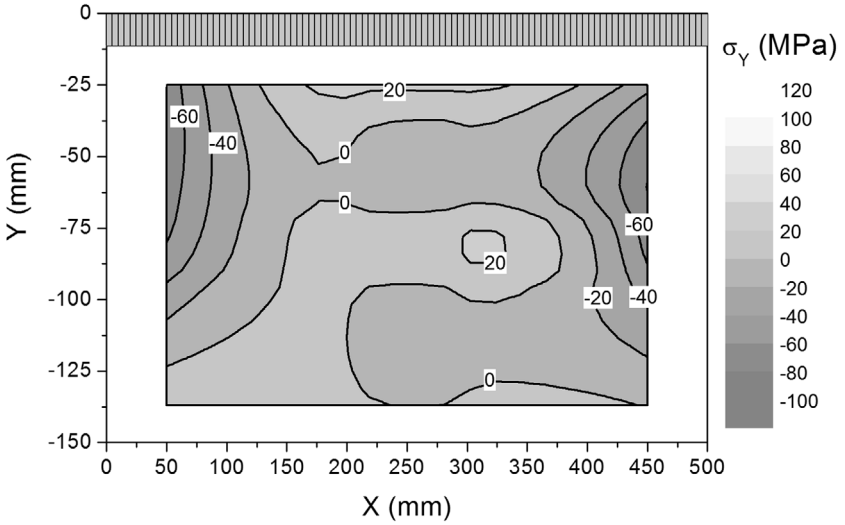

Figure 11. The map showing the σ_y (perpendicular to the weld seam) component distribution on the investigated plate.

do not vary much (especially for tensile stresses). In the case of anisotropic material, such procedure cannot be applied, rotation of the probe away from the structure dependent initial magnetic easy axis results in the deformation of the BE intensity distribution and the reliability of the measurements diminishes. The effect may be to some degree counterbalanced by modifying the amplitudes of the magnetising currents, yet such modification would require new calibration (as the modification would be dependent on the level of anisotropy of the steel in question) to give reliable results. In such a case the σ_1 and σ_2 values have to be calculated on the basis of ε_1 and ε_2 components obtained on the basis of three strain components (ε_a, ε_b and ε_c), at least one of which is determined from the approximated calibration curve.

In order to do calculate ε_1 and ε_2 one can use the general transformation rule allowing for calculation of the components of the stress state in the rotated reference system:

$$\varepsilon_{x'} = \varepsilon_x \cos^2 \alpha_{x'} + \varepsilon_y \sin^2 \alpha_{x'} + \gamma_{xy} \sin \alpha_{x'} \cos \alpha_{x'} \qquad (5)$$

We can assume the x and y axes to be parallel to the main strain axes and use the transformation rule three times for the values of the rotation angle equal to $-45°$, $45°$ (such

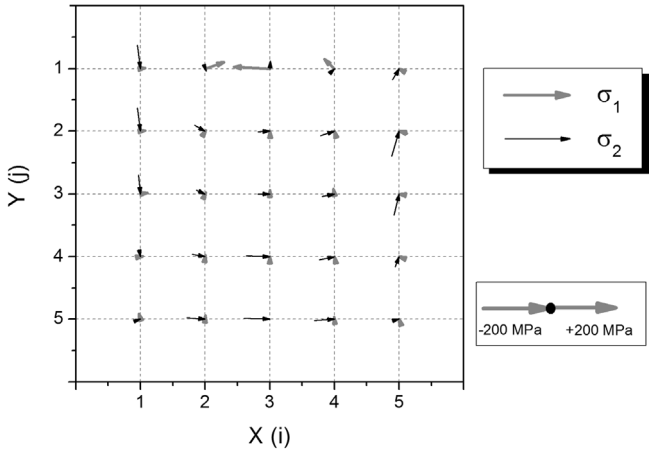

Figure 12. The vector plot showing the distribution of the main stress components (σ_1 and σ_2)—upper side of the plate.

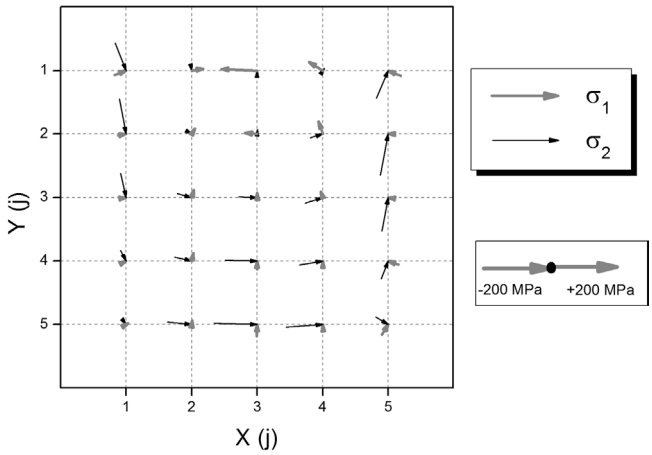

Figure 13. The vector plot showing the distribution of the main stress components (σ_1 and σ_2)—bottom side of the plate.

orientations represent the values obtained for the x and y axes of the apparatus) and an arbitrarily chosen angle α. The geometry is sketched in figure 14, where a, b, c axes are parallel to the chosen strain components. We can set $\alpha = 0°$ and then the transformation rules take the form:

$$\varepsilon_{-45} = \frac{1}{2}(\varepsilon_1 + \varepsilon_2) + \frac{1}{2}(\varepsilon_1 - \varepsilon_2)\cos(-90°) + \frac{1}{2}\gamma_{12}\sin(-90°)$$

$$\varepsilon_{45} = \frac{1}{2}(\varepsilon_1 + \varepsilon_2) + \frac{1}{2}(\varepsilon_1 - \varepsilon_2)\cos(90\,°) + \frac{1}{2}\gamma_{12}\sin(90°)$$

$$\varepsilon_0 = \frac{1}{2}(\varepsilon_1 + \varepsilon_2) + \frac{1}{2}(\varepsilon_1 - \varepsilon_2)\cos(0\,°) + \frac{1}{2}\gamma_{12}\sin(0°)$$

Elementary calculations than lead to the following result: $\varepsilon_1 = \varepsilon_0$; $\varepsilon_2 = \varepsilon_{-45} + \varepsilon_{45} - \varepsilon_0$. One can note that with such a choice of the strain components one can also obtain the result directly from the strain invariant $\varepsilon_2 + \varepsilon_1 = \varepsilon_{-45} + \varepsilon_{45}$.

The results of the stress measurements with the help of the described method have been validated by comparing with the results of the x-ray diffraction analysis—the measurement were performed exactly at the [1, 3] points on both sides of

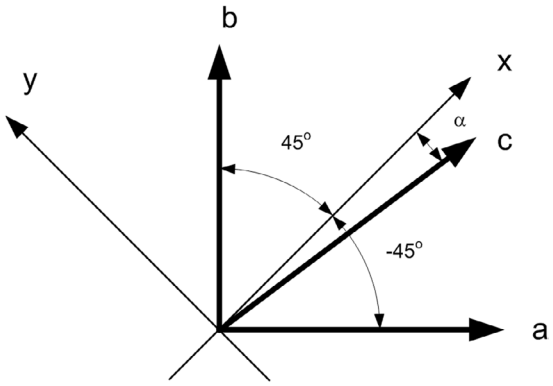

Figure 14. The sketch of geometry used for the main strains determination in the case of main axis orientation equal to 45°.

Table 3. Stress state at the [1, 3] point (both sides) as determined by the x-ray measurements.

	X-ray diffraction	
	σ_x (MPa)	σ_y (MPa)
Up	99 ± 2	37 ± 6
Bottom	79 ± 4	16 ± 6

the plate. The x-ray method gave the values of the σ_x and σ_y components—the results of those investigations are presented in table 3.

One may observe that the results obtained with both methods are qualitatively similar. One obtains the strong tensile stress parallel to the weld seam and much smaller one in the perpendicular direction. There is a difference in the sign of the σ_2 stresses obtained for the bottom side, yet they are both close to zero. Concluding one may state that the magnetic method gives reliable information on the stress level distribution.

7. Summary

In the paper a concise description of the measurement device for a fast determination of the stress state in industrial components made of steel, was given. The measurement procedure was illustrated by the results of stress distribution investigations performed on the butt welded plates. The stress state was determined on the basis of the BE signal intensity angular distribution measurements. The novelty of the described procedure is due to the fact of application of a four pole probe, allowing for the automated change of the magnetisation axis by a determined angle step and BE intensity measurements for all the set magnetisation orientations. Such an automation reduces the measurement time significantly, allowing to perform the measurements with 10° angular step (full rotation) in about 30 s.

The stress determination procedure with the help of the measured BE intensity distribution is based on a set of operations that can be easily automated—by applying an adequate file naming convention one can reduce the user's contribution to specifying the calibration data file, and the data file folder

location. On the basis of the BE signal intensity distributions and reverse calibration curves, the strain angular distributions in every point are calculated. The calibration curves are measured for the easy and hard magnetisation axes and for the intermediate orientations the adequate curves are interpolated. During the measurements the probe should be oriented (relative to the easy axis) in the same way as during the calibration. The strain angular distribution is used for the determination of two strain components (along calibration axes) and the strain main axis orientation. Those values allow for the determination of the main stresses (the main stress axis being parallel to that of strain). The results of the measurements may be illustrated with the help of commonly used maps of stress components (parallel to plate edges) spatial distribution. It is however more illustrative to use the vector maps showing both the main stress components magnitude and orientation. The very short measurement time, possibility of almost complete automation of the process, and the completeness of the obtained information provide expectation that the as-presented method will soon be implemented in the industrial environment.

Acknowledgments

This study was partly funded by Polish National Centre for Research and Development (Grant MAGSTRESS Number PBS1/A9/14/2012).

References

[1] Lu J (ed) 1996 *Handbook of Measurement of Residual Stresses* (Liburn: The Fairmont Press)
[2] Pasley R L 1970 Barkhausen effect—an indication of stress *Mater. Eval.* **28** 157–61
[3] Santa-aho S, Sorsa A, Hakanen M, Leiviska K, Vippola M and Lepisto T 2014 Barkhausen noise-magnetizing voltage sweep measurement in evaluation of residual stress in hardened components *Meas. Sci. Technol.* **25** 085602
[4] Piotrowski L, Augustyniak B, Chmielewski M and Kowalewski Z 2010 Multiparameter analysis of the Barkhausen noise signal and its application for the assessment of plastic deformation level in 13HMF grade steel *Meas. Sci. Technol.* **21** 115702
[5] Augustyniak B 2003 *Magneto-Elastic Phenomena and Their Applications in Non-Destructive Evaluation of Materials* (Gdansk: Gdansk University of Technology)
[6] Capo-Sanchez J, Perez-Benitez J and Padovese L R 2007 Analysis of the stress dependent magnetic easy axis in ASTM 36 steel by the magnetic Barkhausen noise *NDT E Int.* **40** 168–172
[7] Caldas-Morgan M and Padovese L R 2012 Fast detection of the magnetic easy axis on steel sheet using the continuous rotational Barkhausen method *NDT E Int.* **45** 148–55
[8] Espina-Hernandez J H, Perez-Benıtez J A, Caleyo F, Baudin T, Helbert A L and Hallen J M 2013 Barkhausen noise measurements give direct observation of magneto-crystalline anisotropy energy in ferromagnetic polycrystals *J. Phys. D: Appl. Phys.* **46** 392001
[9] Piotrowski L, Chmielewski M, Augustyniak B, Maciakowski P and Prokop K 2015 Stress anisotropy characterization with the help of Barkhausen effect detector with adjustable magnetic field direction *Int. J. Appl. Electromagn.* **48** 163–170
[10] Augustyniak M, Augustyniak B, Piotrowski L and Chmielewski M 2015 Determination of magnetisation conditions in a double-core barkhausen noise measurement set-up *J. Nondestruct. Eval.* **34** 16
[11] Sablik J M, Smith M Q, Waldhart C J, McKee D A and Augustyniak B 1998 The effects of biaxial stress on Barkhausen noise signals when the magnetic field is noncoaxial with the stress *J. Appl. Phys.* **84** 6239–49
[12] Hristoforou E, Vourna P, Ktena A and Svec P 2016 On the Universality of the dependence of magnetic parameters on residual stresses in steels *IEEE Trans. Magn.* **52** 6201106
[13] Krause T W, Clapham L, Pattantyus A and Atherton D L 1996 Investigation of the stress-dependent magnetic easy axis in steel using magnetic Barkhausen noise *J. Appl. Phys.* **79** 4242–52
[14] Yelbay H I, Cam I and Gur C H 2010 Non-destructive determination of residual stress state in steel weldments by magnetic Barkhausen noise technique *NDT E Int.* **43** 29–33
[15] Vourna P, Hervoches Ch, Vrána M, Ktena A and Hristoforou E 2015 Correlation of magnetic properties and residual stress distribution monitored by x-ray and neutron diffraction in welded AISI 1008 steel sheets *IEEE Trans. Magn.* **51** 6200104
[16] Vourna P, Ktena A, Tsakiridis P E and Hristoforou E 2015 An accurate evaluation of the residual stress of welded electrical steels with magnetic Barkhausen noise *Measurement* **71** 31–45
[17] Sambamurthy E, Dutta S, Panda A K, Mitra A and Roy R K 2014 Evaluation of post-weld heat treatment behavior in modified 9Cr–1Mo steel weldment by magnetic Barkhausen emission *Int. J. Press. Vessels. Pip.* **123–4** 86–91
[18] Lindgren M and Lepisto T 2002 Application of Barkhausen noise to biaxial residual stress measurements in welded steel tubes *Mater. Sci. Tech.* **18** 1969–76
[19] Paradowska A M, Price J W H, Finlayson T R, Lienert U, Walls P and Ibrahim R 2009 Residual stress distribution in steel buttwelds measured using neutron and synchrotron diffraction *J. Phys.: Condens. Matter* **21** 124213
[20] Liang W, Murakawa H and Deng D 2015 Investigation of welding residual stress distribution in a thick-plate joint with an emphasis on the features near weld end-start *Mater. Des.* **67** 303–12